

## Test of the innermost inner core models using broadband PKIKP travel time residuals

A. Cao<sup>1</sup> and B. Romanowicz<sup>1</sup>

Received 17 January 2007; revised 9 March 2007; accepted 26 March 2007; published 25 April 2007.

[1] Two different innermost inner core (IMIC) models have recently been proposed, each with different radii and different orientation and strength of anisotropy. In order to test these IMIC models, we have systematically assembled a high quality dataset of broadband PKIKP data in the epicentral distance range of 150° to 180°. Our new dataset consists of ~1,100 individually measured absolute PKIKP arrival times. Also, PKIKP bottoming points and ray paths in the inner core are well distributed in the east-west and north-south hemispheres. We invert this dataset for two layer models of anisotropy in the inner core and compare the fits obtained with those predicted from the existing IMIC models. Our results show that, if there is an IMIC, its radius is most likely around ~500 km rather than the ~300 km originally proposed, and is in better agreement with the layering in the inner core based on PKIKP waveform modeling. **Citation:** Cao, A., and B. Romanowicz (2007), Test of the innermost inner core models using broadband PKIKP travel time residuals, *Geophys. Res. Lett.*, 34, L08303, doi:10.1029/2007GL029384.

### 1. Introduction

[2] Since the first evidence for inner core anisotropy was presented [Morelli *et al.*, 1986; Woodhouse *et al.*, 1986], increasingly complex models have been proposed. It has been documented that anisotropy increases with depth in the inner core [Vinnik *et al.*, 1994; Creager, 1999; Song, 1996], and that it is much weaker in the quasi-eastern than in the quasi-western hemisphere [Tanaka and Hamaguchi, 1997; Creager, 1999]. At the top of the inner core (<~100 km), P-wave velocity may be isotropic and faster in the quasi-eastern hemisphere than in the quasi-western hemisphere [Niu and Wen, 2001; Garcia, 2002; Cao and Romanowicz, 2004; Garcia *et al.*, 2004].

[3] The above complexity was questioned by several authors [Bréger *et al.*, 2000; Romanowicz *et al.*, 2003; Ishii *et al.*, 2002]. The complex lateral variations in P-wave velocity could be due to mantle, and possibly outer core heterogeneity [Bréger *et al.*, 2000; Romanowicz *et al.*, 2003]. Ishii *et al.* [2002] suggested that there need not be an isotropic layer at the top of the inner core and that both body wave and normal mode observations can be explained by a model with constant anisotropy in the inner core.

[4] More recently, the existence of an innermost inner core (IMIC), within which the anisotropic characteristics are distinct, was proposed, respectively based on body wave

[Ishii and Dziewoński, 2002] (hereinafter referred to as ID02) and normal mode data [Beghein and Trampert, 2003] (hereinafter referred to as BT03). However, the structures proposed are inconsistent: not only are the radii of the IMIC different (~300 km (ID02) versus ~400 km (BT03)), but, more importantly, so are the slowest directions of anisotropy: in one model, the slowest direction is ~45° with respect to the earth's spin axis (ID02), the other is along the spin axis (BT03). Cormier and Stroujkova [2005] tested the IMIC model of ID02 using PKIKP waveform modeling and suggested a much larger radius (~500 km). Because the existence of the suggested IMIC is thought to be closely related to the early stages of inner core formation, it is important to try and clarify this inconsistency through further study.

[5] The ID02 dataset is derived from the International Seismological Center (ISC) bulletins, and their study relies on the statistical analysis of a large noisy dataset. On the other hand, BT03 used normal mode data, the resolution of which decreases towards the center of the inner core. In this paper, we assemble a new dataset of absolute PKIKP (Figure 1) travel time residuals, which are measured on high quality digital broadband seismograms recorded in global and local seismic networks (e.g., GSN, GEOSCOPE, and PASSCAL), to explore the seismic anisotropy in the central part of the inner core.

### 2. Data, Method, and Results

[6] We systematically downloaded broadband vertical component seismograms ( $M_w > 6.0$ , depth > 0 km) from the IRIS Data Management Center (DMC) corresponding to the epicentral distance range 150° to 180°, and for the time period 1990 to 2003, for which the relocated EHB event catalog is available [Engdahl *et al.*, 1998]. Thousands of seismograms recorded at global and regional networks were collected. Absolute PKIKP travel time residuals were measured with respect to the reference seismic model PREM [Dziewoński and Anderson, 1981], using relocated hypocenter and origin time as given in the EHB catalog, and correcting for ellipticity [Dziewoński and Gilbert, 1976]. We also conducted corrections for mantle heterogeneities using a P-wave global tomography model [Karason and van der Hilst, 2001].

[7] We consider a 40-second time window, centered on the corrected theoretical PKIKP arrival time, and inspect original broadband seismograms individually without any filtering (Figures 1b, 1c, and 1d). Only two kinds of seismograms are kept for further PKIKP arrival time picking, those for which: (1) the background noise is very flat and the onset of PKIKP is very sharp (Figures 1c and 1d); (2) the background noise is not so flat as in (1), but it

<sup>1</sup>Berkeley Seismological Lab, University of California, Berkeley, California, USA.

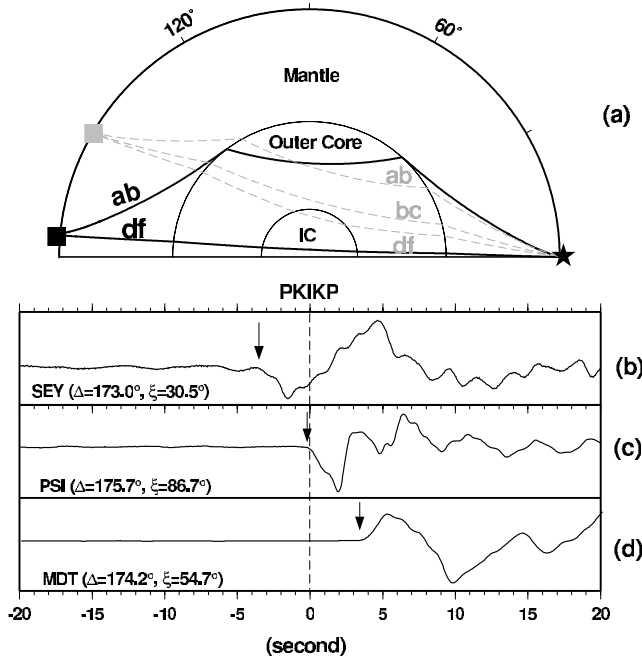


**Figure 1.** (a) Ray paths of PKIKP and PKP phases. The black solid line shows the ray path of PKIKP, which is used in this study. The grey dashed lines show ray paths of PKP which are not suitable to this study. The event and stations are indicated by a star and squares, respectively. (b, c, d) Examples of PKIKP absolute travel time residual measurement. Seismograms are aligned with respect to the dashed line, which marks theoretical arrival times with respect to PREM after ellipticity and mantle corrections. Station names, epicentral distances, angles between ray path, and the earth spinning axis are given. Arrows are the picked PKIKP arrival times. Figure 1b shows South Sandwich Islands event ( $M_w = 6.6$ , depth = 37.5 km, 12/28/1991). Figure 1c shows Northern Peru Event ( $M_w = 6.7$ , depth = 97.0 km, 05/02/1995). Figure 1d shows New Zealand event ( $M_w = 7.1$ , depth = 41.0 km, 02/05/1995).

fluctuates regularly before the clear onset of PKIKP (Figure 1b). Then we zoom in the record by a factor of  $\sim 5$  around the PKIKP onset time, to read its arrival time. The reading error is within  $\pm 0.3$  second. We thus obtain a dataset of  $\sim 1100$  high quality travel time residual measurements (Figure 2). In particular, in the nearly antipodal epicentral distance range of  $170^\circ$  to  $180^\circ$  (Figures 2c and 2d), we have  $\sim 264$  measurements. Bottoming points and ray paths of PKIKP are well distributed in the east-west or north-south hemispheres (see Figure S1 of the auxiliary material).<sup>1</sup>

[8] For transversely isotropic inner core models [Woodhouse *et al.*, 1986], the PKIKP travel time residual is expressed as:

$$\delta t = - \int \frac{\delta v}{v^2} ds = - \int \frac{A \cos^2 \xi + B \cos^4 \xi}{v} ds \quad (1)$$

where  $A = 2\beta - \gamma$ ,  $B = \frac{\alpha}{2} + \gamma - 2\beta$ ,  $v$  is the average P-wave velocity in the inner core equatorial plane,  $\delta v$  is the velocity perturbation as a function of angle  $\xi$  formed by the ray path in the inner core and the earth's rotation axis, and  $s$  is the PKIKP ray length in the inner core.  $\alpha$ ,  $\beta$ , and  $\gamma$  are three anisotropic parameters, related to the standard radial anisotropy parameters  $A$ ,  $C$ ,  $F$ ,  $L$ ,  $N$  [Love, 1927] by:

$$\alpha = \frac{(C - A)}{\rho v^2}, \quad \beta = \frac{(L - N)}{\rho v^2}, \quad \text{and} \quad \gamma = \frac{(A - 2N - F)}{\rho v^2} \quad (2)$$

where  $\rho$  is the average density in the inner core.

[9] For polar PKIKP paths ( $\xi = 0$ ), the sign of  $\delta t$  is controlled by the anisotropic parameter  $\alpha$  in equation (1). If  $\alpha$  is positive,  $\delta t$  is negative, reflecting the fact that the P-wave velocity is faster along polar than equatorial paths. If  $\alpha$  is negative, then the P-wave velocity is slower along polar paths. Unlike in ID02's model, the anisotropic parameter  $\alpha$  changes sign (from positive to negative toward the center) around a radius of 400 km, in the BT03 model. This implies a different kind of IMIC.

[10] In the realistic Earth's inner core, the seismic velocity structure is most likely not purely anisotropic [Niu and Wen, 2001; Garcia, 2002; Cao and Romanowicz, 2004; Garcia *et al.*, 2004], and the influence of mantle heterogeneities cannot be completely ruled out [Bréger *et al.*, 2000; Romanowicz *et al.*, 2003]. Thus, equation (1) needs to be modified with a non-anisotropic shift term  $\eta_0$ :

$$\delta t' = \delta t + \eta_0 \quad (3)$$

[11] In order to test seismic models of ID02 and BT03, we calculate the predicted absolute PKIKP travel time residuals with equation (3) using the parameters of their respective anisotropic models.  $\eta_0$  is the average value at  $\xi = \sim 90^\circ$  in each epicentral distance range (Figure 2).

[12] We divide our observations into four epicentral distance ranges (Figure 2), corresponding to different depths of penetration of PKIKP in the inner core. In the epicentral distance range  $173^\circ$  to  $180^\circ$ , which corresponds to rays that sample the very center of the inner core, we confirm the trend observed by ID02, namely that the travel time residuals are maximum at intermediate angles  $\xi$ , decreasing both for polar ( $\xi \sim 0$ ) and for equatorial ( $\xi \sim 90^\circ$ ) paths. This means that the slowest P-wave velocity direction is not along the equatorial plane. This is why ID02 proposed the existence of an IMIC with a radius of  $\sim 300$  km and a slowest direction oriented at  $\sim 45^\circ$  with respect to the earth's rotation axis. However, our dataset indicates that the same trend is also present at shorter epicentral distances (Figures 2b, 2c, and 2d). More importantly, in the epicentral distance range  $165^\circ$  to  $180^\circ$ , neither ID02 model nor BT03 model can fit our observations. This fact suggests two possibilities: (1) there is an IMIC, but its anisotropic character is different from that in ID02 and BT03; (2) there is no IMIC.

[13] First, we assume the existence of an IMIC. While keeping the upper layer anisotropic structure fixed, as given in ID02 (bulk constant anisotropy) and in BT03 (depth-dependent), respectively, we correct the observed PKIKP travel time residuals ( $\delta t'$ ) (Figure 2) by subtracting  $\eta_0$  and  $\delta t_{upper}$  (contributed by the upper layer) from equation (3) and then invert for the anisotropic parameters  $A$  and  $B$

<sup>1</sup>Auxiliary materials are available in the HTML. doi:10.1029/2007GL029384.

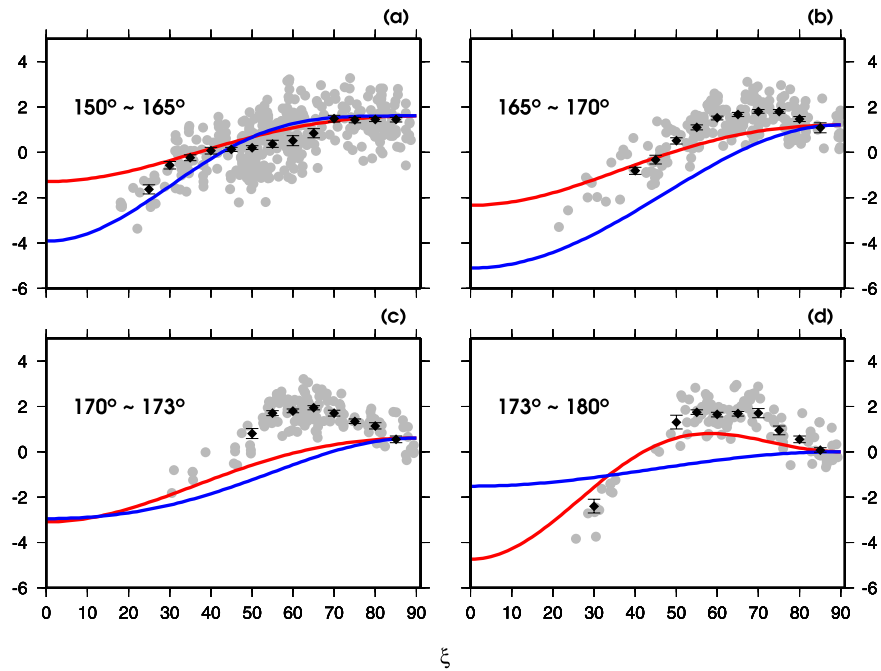


**Figure 2.** Absolute PKIKP travel time residuals as a function of  $\xi$ . Grey dots are the measured residuals with respect to PREM model after ellipticity and mantle corrections. Red and blue lines are theoretical residuals calculated from ID02 and BT03 models. Black diamonds are means of the residuals in  $10^\circ$  bins of  $\xi$  when the number of measurements is not less than 10, with error bars corresponding to standard deviation of the mean. The epicentral distance ranges are as indicated. The range  $173^\circ$  to  $180^\circ$  was used in ID02, and corresponds to rays bottoming at a radius of  $\sim 300$  km; the range  $170^\circ$  to  $173^\circ$  corresponds to a radius of  $\sim 300$ – $400$  km, whereas the range  $165^\circ$  to  $170^\circ$  corresponds to a radius of  $\sim 400$ – $550$  km. We group our observations in Figure 2a for distances shorter than  $165^\circ$ .

(equation (1)) in the IMIC. It is clear that the constrained anisotropy in the IMIC depends mildly on the anisotropic structure in the upper layer of the inner core (Figure 3). If the upper layer has the bulk constant anisotropic structure as used in ID02, the optimal IMIC radius inverted from our dataset is  $\sim 480$  km, and the corresponding variance reduc-

tion is 0.89 (Figure 3a). In contrast, the IMIC radius (300 km) suggested in ID02 is so small that the corresponding variance reduction is very low ( $\sim 0.3$ ). If the upper layer has the depth-dependent anisotropic structure as suggested in BT03, the optimal IMIC radius inverted from our dataset is  $\sim 530$  km, and the corresponding variance

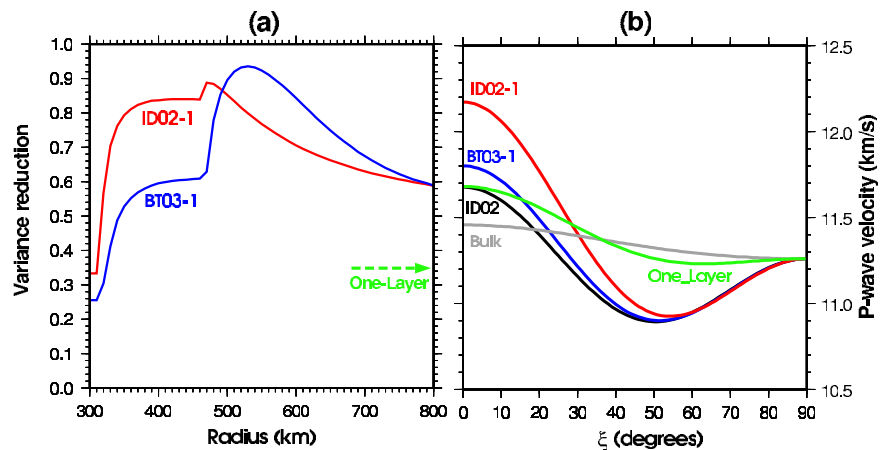


**Figure 3.** Constraints on the IMIC P-wave velocity anisotropy. (a) Variance reduction with respect to the IMIC radius for the inversion based on our measured PKIKP travel time residuals. Here we assume a two-layer inner core model. The upper layer anisotropy is that of ID02 (red line, ID02-1) or BT03 (blue line, BT03-1). In contrast, the dashed green arrow denotes the variance reduction with respect to the one-layer inner core model. (b) Inverted P-wave velocity anisotropy in the IMIC based on ID02-1 (red) and BT03-1 (blue), respectively. One-layer inner core anisotropic model (i.e., no IMIC) obtained by inversion (green) is also shown. The black line is the IMIC anisotropy suggested in ID02, and the grey line is the reference bulk constant anisotropic structure of ID02.

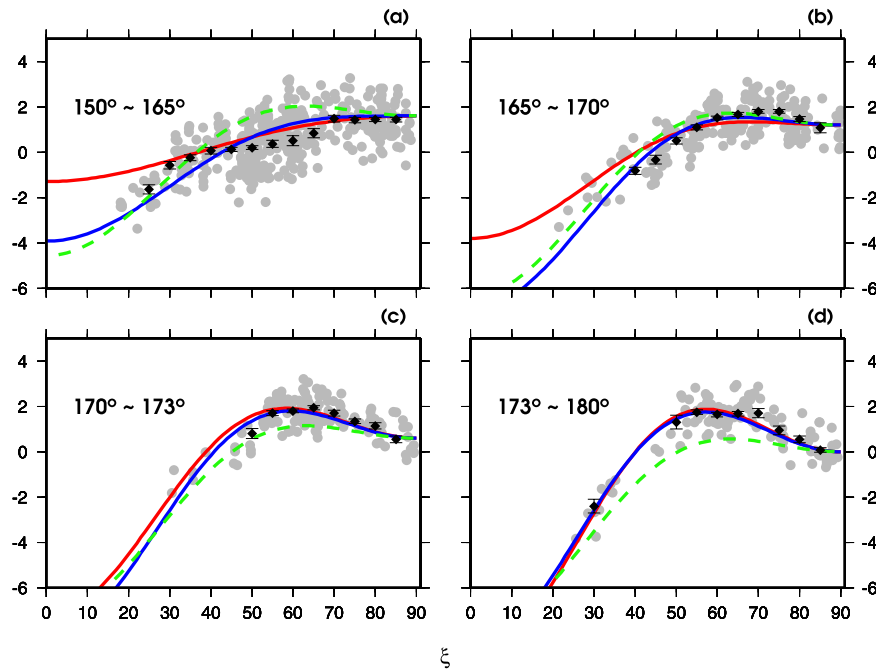


**Figure 4.** Theoretical PKIKP travel time residuals as a function of  $\xi$ , which include  $\delta t_{IMIC}$  (contributed by our inverted IMIC),  $\delta t_{upper}$  (contributed by the upper layer), and  $\eta_0$ . The red and blue lines correspond to the best fitting IMIC models with a bulk constant (ID02-1) and a depth-dependent (BT03-1) anisotropic upper layer, respectively. The dashed green line corresponds to a one-layer (i.e., no IMIC) anisotropic inner core model. The grey dots are data as in Figure 1.

reduction is 0.94 (Figure 3a). Thus an IMIC with a depth-dependent anisotropic upper layer fits our dataset better. In both cases, the constrained IMIC radii are compatible with the radius suggested by *Cormier and Stroujkova* [2005] on the basis of PKIKP waveform modeling. In addition to the radius, the inverted IMIC anisotropic character is also mildly dependent on the upper layer anisotropy. Exploring this further would require data at epicentral distances shorter than  $165^\circ$ . The constrained slowest directions are  $\sim 50^\circ$  and  $\sim 55^\circ$ , when considering a ID02 or BT03 upper layer, respectively (Figure 3b). And the constrained P-wave velocities along the axis of the earth's rotation are 4.2% and 1.1% faster than that suggested in ID02, respectively (Figure 3b).

[14] Second, if there is no IMIC in the inner core, the variance reduction for a one-layer model is small (0.35). A constant anisotropy, one-layer, model can provide good fits to our observations in the epicentral distance range of  $165^\circ$  to  $170^\circ$ , but in other ranges, particularly from  $173^\circ$  to  $180^\circ$ , it does not (Figure 4). Both of the inverted “two-layer” IMIC models fit our observations very well in the epicentral distance ranges of  $173^\circ$  to  $180^\circ$  and  $170^\circ$  to  $173^\circ$ . In the other two epicentral distance ranges ( $150^\circ$  to  $165^\circ$  and  $165^\circ$  to  $170^\circ$ ), however, the model with an upper layer as in BT03-1 fits our dataset better (Figure 4). This suggests that the anisotropic structure in the upper part of the inner core most likely changes with depth.

### 3. Discussion

[15] Even though we use a relocated catalog and apply mantle corrections, the influence of mislocations and mantle heterogeneities on our absolute PKIKP arrival time resid-

uals cannot be removed completely. This is likely one of the main reasons for the scatter observed in our data in individual epicentral distance bins. However, this shortcoming should be well compensated by the global distribution of PKIKP bottoming points. As in all previous global body wave studies, most events are in subduction zones and most stations are on continents (see Figure S1). This kind of combination most likely biases all our measurements in a similar way. Because we mainly focus on trends rather than absolute values of residuals, this is not a serious problem for us. In fact, in all our epicentral distance ranges (Figures 2 and 4), the average trends of absolute PKIKP travel time residuals as a function of  $\xi$  are clear. In addition, the suggested hemispherical velocity perturbations are small ( $\sim 0.8\%$ ) in the uppermost inner core ( $\sim 150$  km) [*Niu and Wen*, 2001; *Garcia et al.*, 2004], and so the resulting influence on our PKIKP travel time residuals are negligible.

[16] Even though two-layer models with IMIC explain our observations well, we cannot rule out more complicated anisotropic structures in the inner core. The fact that the maximum of residuals is found at intermediate angles  $\xi$  (Figures 2 and 4) means that the slowest P velocity direction is not along the equatorial plane. Two previously suggested mechanisms [*Yoshida et al.*, 1996; *Wenk et al.*, 2000] imply that, close to the equatorial plane, iron crystals may be horizontally well aligned by the flow caused by non-hydrostatic or convection-related deformations. This suggests that in the nearly antipodal epicentral distance range, the slowest direction would be between  $0^\circ$  and  $90^\circ$  rather than along the equatorial plane ( $90^\circ$ ). For these kinds of possible mechanisms of inner core anisotropy, however,

quantitative modeling is challenging because of the inadequate data distribution.

#### 4. Conclusion

[17] Our independent dataset of absolute PKIKP travel time residuals confirms that an IMIC is needed to explain the trends at near-antipodal epicentral distances. The constrained radius and velocity anisotropy of the IMIC depend mildly on the suggested structure in the upper layer. The IMIC radius is larger ( $\sim 500$  km) than proposed in ID02 and its slowest direction may be between  $50^\circ$  and  $55^\circ$ . Neither ID02 nor BT03 IMIC models fit our observations well, however the layering obtained from waveform modeling is compatible with our data.

[18] **Acknowledgments.** We thank the following data center and networks for providing the high quality data in this study: IRIS-DMC, GSN, GEOSCOPE, and PASSCAL. We are grateful to Xiaodong Song and an anonymous reviewer for their constructive comments. This work was supported by NSF grant EAR-0308750. This is Berkeley Seismological Laboratory contribution 07-02.

#### References

- Beghein, C., and J. Trampert (2003), Robust normal mode constraints on inner core anisotropy from model space search, *Science*, *299*, 552–555.
- Bréger, L., H. Tkalcic, and B. Romanowicz (2000), The effect of  $D''$  on PKP (AB-DF) travel time residuals and possible implications for inner core structure, *Earth Planet. Sci. Lett.*, *175*, 133–143.
- Cao, A., and B. Romanowicz (2004), Hemispherical transition of seismic attenuation at the top of the Earth's inner core, *Earth Planet. Sci. Lett.*, *228*, 243–253.
- Cormier, V., and A. Stroujkova (2005), Waveform search for the innermost inner core, *Earth Planet. Sci. Lett.*, *236*, 96–105.
- Creager, K. C. (1999), Large-scale variations in inner core anisotropy, *J. Geophys. Res.*, *104*, 23,127–23,139.
- Dziewoński, A. M., and D. L. Anderson (1981), Preliminary reference Earth model, *Phys. Earth Planet. Inter.*, *25*, 297–356.
- Dziewoński, A. M., and F. Gilbert (1976), The effect of small aspherical perturbations on travel times and a re-examination of the corrections for ellipticity, *Geophys. J. R. Astron. Soc.*, *44*, 7–17.
- Engdahl, E. R., R. D. van der Hilst, and R. P. Buland (1998), Global teleseismic earthquake relocation with improved travel times and procedures for depth determination, *Bull. Seismol. Soc. Am.*, *88*, 722–743.
- Garcia, R. (2002), Constraints on upper inner-core structure from waveform inversion of core phases, *Geophys. J. Int.*, *150*, 651–664.
- Garcia, R., S. Chevrot, and M. Weber (2004), Nonlinear waveform and delay time analysis of triplicated core phases, *J. Geophys. Res.*, *109*, B01306, doi:10.1029/2003JB002429.
- Ishii, M., and A. M. Dziewoński (2002), The innermost inner core of the Earth: Evidence for a change in anisotropic behavior at the radius of about 300km, *Proc. Natl. Acad. Sci. U. S. A.*, *22*, 14,026–14,030.
- Ishii, M., A. M. Dziewoński, J. Tromp, and G. Ekström (2002), Joint inversion of normal mode and body wave data for inner core anisotropy: 2. Possible complexities, *J. Geophys. Res.*, *107*(B12), 2380, doi:10.1029/2001JB000713.
- Karason, H., and R. D. van der Hilst (2001), Improving global tomography models of P-wavespeed: 1. Incorporation of differential times for refracted and diffracted core phases (PKP, Pdiff), *J. Geophys. Res.*, *106*, 6569–6587.
- Love, A. E. H. (1927), *A Treatise on the Theory of Elasticity*, 4th ed., Cambridge Univ. Press, New York.
- Morelli, A., A. M. Dziewoński, and J. H. Woodhouse (1986), Anisotropy of the inner core inferred from PKIKP travel times, *Geophys. Res. Lett.*, *13*, 1545–1548.
- Niu, F., and L. Wen (2001), Hemispherical variations in seismic velocity at the top of the Earth's inner core, *Nature*, *410*, 1081–1084.
- Romanowicz, B., H. Tkalcic, and L. Bréger (2003), On the origin of complexity in PKP travel time data from broadband records, in *Earth's Core: Dynamics, Structure, Rotation, Geodyn. Ser.*, vol. 31, edited by V. Dehant et al., pp. 31–44, AGU, Washington, D. C.
- Song, S. (1996), Anisotropy in central part of inner core, *J. Geophys. Res.*, *101*, 16,089–16,097.
- Tanaka, S., and H. Hamaguchi (1997), Degree one heterogeneity and hemispherical variation of anisotropy in the inner core from PKP (BC)-PKP (DF) times, *J. Geophys. Res.*, *102*, 2925–2939.
- Vinnik, L., B. Romanowicz, and L. Bréger (1994), Anisotropy in the center of the inner core, *Geophys. Res. Lett.*, *21*, 1671–1674.
- Wenk, H. R., J. R. Baumgardner, R. A. Lebensohn, and C. N. Tome (2000), A convection model to explain anisotropy of the inner core, *J. Geophys. Res.*, *105*, 5663–5677.
- Woodhouse, J. H., D. Giardini, and X. D. Li (1986), Evidence for inner core anisotropy from free oscillations, *Geophys. Res. Lett.*, *13*, 1549–1552.
- Yoshida, S., I. Sumita, and M. Kumazawa (1996), Growth model of the inner core coupled with the outer core dynamics and the resulting elastic anisotropy, *J. Geophys. Res.*, *101*, 28,085–28,103.

A. Cao and B. Romanowicz, Berkeley Seismological Lab, University of California, Berkeley, 215 McCone Hall, Berkeley, CA 94720, USA. (acao@seismo.berkeley.edu)